

## EFFECT OF POSITIVE GATE STRESSING ON THE RECOVERABLE COMPONENT OF NEGATIVE-BIAS TEMPERATURE INSTABILITY

A. A. BOO, D. S. ANG<sup>+</sup>, Z. Q. TEO, AND C. M. NG<sup>\*</sup>

Nanyang Technological University, School of Electrical and Electronic Engineering; Singapore 639798;  
<sup>\*</sup>GLOBALFOUNDRIES Singapore Pte. Ltd., Singapore 738406 (<sup>+</sup>E-mail: [edsang@ntu.edu.sg](mailto:edsang@ntu.edu.sg))

### I. INTRODUCTION AND NOVELTY OF THIS WORK

Negative-bias temperature instability (NBTI) has attracted considerable attention due to its significant impact on the performance of the P-MOSFET. It has been shown that NBTI induced threshold voltage shift ( $|\Delta V_t|$ ) comprises a recoverable (R) and a relatively permanent (P) component<sup>1-3</sup>. However, nature of the underlying defects remains unclear, although temperature dependence study<sup>3</sup> has revealed distinct activation energies, implying different defect nature of the two components. A current viewpoint ascribes R to preexisting oxide traps and high-field induced oxide trap generation, suggesting that it is an *extrinsic* effect. In this work, we reveal an interesting effect of a positive gate voltage ( $V_g$ ) stress, applied prior to NBTI, on the subsequent R component. A prior positive  $V_g$  stress is shown to reduce R. Most importantly, the reduction becomes more severe at a later stage when oxide trap generation is relatively significant, as evidenced by a substantial increase in the stress induced leakage current (SILC). This observation does not support the notion that R is related to preexisting oxide traps and stress induced oxide trap generation.

### II. EXPERIMENTAL DETAILS

Test devices were p<sup>+</sup> polysilicon gate P-MOSFETs with 1.8 nm oxynitride gate prepared via decoupled plasma nitridation. NBTI test was carried out at a gate stress voltage of  $-1.8$  V (oxide field  $\sim 7.7$  MV/cm) and at a temperature of  $100$  °C. At specific intervals,  $I_d$ - $V_g$  curve was measured using an ultrafast switching method<sup>4</sup>. The short delay of  $\sim 60$  ns not only minimizes recovery significantly, it suppresses cumulative recovery during  $I_d$ - $V_g$  measurement<sup>5</sup>. Device degradation was measured in terms of  $|\Delta V_t|$ , extracted at a constant drain current.

### III. RESULTS AND DISCUSSION

#### A. "Cyclic" Nature of Dynamic NBTI

Fig. 1 depicts typical evolution of  $|\Delta V_t|$  across the stress and recovery (S&R) cycle, showing apparent fast and slow recovery phases. The amount of  $|\Delta V_t|$  recovery per cycle,  $|\Delta V_t|^r$  is observed to remain constant over many S&R cycles (Fig. 2(a)). This feature is also evident in Fig. 2(b), in which precise reproduction of the  $|\Delta V_t|^{\text{eor}}$  ( $|\Delta V_t|$  at end-of-recovery) characteristic (solid line) can be achieved by subtracting  $|\Delta V_t|^f$  of the first cycle from  $|\Delta V_t|^{\text{eos}}$  ( $|\Delta V_t|$  at end-of-stress). The constant  $|\Delta V_t|^f$  could not be explained by the hydrogen-transport model<sup>3</sup>, which predicts that  $|\Delta V_t|^f$  would decrease progressively with S&R "cycling" (filled symbol; Fig. 2(a))<sup>3</sup>. It is also observed that the amount of  $|\Delta V_t|$  increase per stress cycle,  $|\Delta V_t|^s$  becomes almost equal to  $|\Delta V_t|^f$  after several S&R cycles. Fig. 3 shows highly repeatable shift of  $|\Delta V_t|$  during stress and recovery over many S&R cycles (thin lines). Although the time dependence of  $|\Delta V_t|$  shift during stress and recovery are different, the values at the end of the stress and recovery period are strikingly similar for all S&R cycles. This observation implies that for a given time window, dynamic

NBTI is always governed by the *same* group of "defects" charged/discharged repeatedly<sup>2,6</sup>. The cyclic behavior strongly suggests the role of preexisting oxide traps.

#### B. Reduction of Cyclic $|\Delta V_t|$ by Positive $V_g$ Stress

To further investigate the nature of the cyclic  $|\Delta V_t|$ , dynamic NBTI was interrupted after 10 cycles and a positive  $V_g$  stress was applied. Thereafter, dynamic NBTI was resumed for another 10 cycles (Fig. 4(a)). Oxide traps were generated during the positive  $V_g$  stress (as inferred from increase in the stress induced leakage current). As a consequence, one would expect to observe a larger cyclic  $|\Delta V_t|$  in the ensuing dynamic NBTI. This inference is, however, not borne out by Fig. 4(b), which depicts, on the contrary, a *decrease* of the cyclic  $|\Delta V_t|$  after the positive  $V_g$  stress.

Fig. 5 shows that the effect of the positive  $V_g$  stress on P is relatively significant in the initial stage (arrow A; Fig. 5(a)) and it decreases at the later stage. On the other hand, the effect on R is relative small initially and it becomes more significant at the later stage. The distinct effects corroborate an earlier inference, based on temperature dependence study<sup>3</sup>, of that the defect nature of R and P are different. Most importantly, the reduction in R occurs at the later stage when oxide trap generation becomes very significant, as can be seen by the substantial increase in the SILC as positive  $V_g$  stress progresses (Fig. 6). An increase in the positive  $V_g$  results in a greater decrease in R (Fig. 7). Greater reduction in R, at a given positive  $V_g$ , is also observed when the stress time is increased (Fig. 8).

#### C. Phenomenological Explanation

In Fig. 5, the faster rise of  $|\Delta V_t|^{\text{eor}}$ , as compared to  $|\Delta V_t|^{\text{eos}}$ , implies that the positive  $V_g$  stress has transformed some fraction of R into a more permanent form. In conjunction with the significant reduction of R at a stage when a substantial amount of oxide traps has been generated, the observations imply that R did not arise out of preexisting oxide defects or defects generated by high field. We speculate that under a negative gate bias, interaction between oxygen lone pairs and holes in the inversion layer enhances polarization of interfacial Si atoms<sup>7</sup> (with no actual breaking of bonds), leading to a  $V_t$  shift that is recoverable. On the other hand, when some of the "precursors" are broken by high-field stress, the amount of recoverable  $V_t$  shift is decreased.

### IV. CONCLUSION

New insights, from a positive  $V_g$  stress applied prior to NBTI, indicate that the recoverable component does not arise from preexisting oxide defects or defects generated by high field stress. A plausible explanation for the nature of the recoverable component is proposed in light of the new experimental findings.

### ACKNOWLEDGEMENT

This work is supported in part by Singapore Ministry of Education under Research Grant MOE2009-T2-1-050.

**REFERENCES:** [1] Grasser *et al.*, IEDM 2007, pp. 801-804; [2] Teo *et al.*, IEEE EDL (31), pp. 269-271, 2010; [3] Teo *et al.*, IEDM 2009, pp. 737-740; [4] Du *et al.*, IEEE EDL (30), pp. 275-277, 2009; [5] Hu *et al.*, IEEE TED, in press; [6] Grasser *et al.*, IEDM 2009, pp. 729-732; [7] Zheng *et al.*, *Prog. Solid State Chem.* (34), pp. 1-20, 2006.

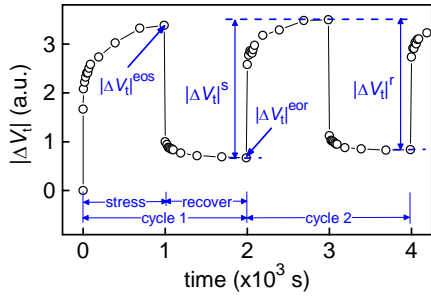


Fig. 1. Evolution of threshold voltage shift,  $|\Delta V_t|$  during typical stress and recovery cycles of a dynamic NBTI experiment.

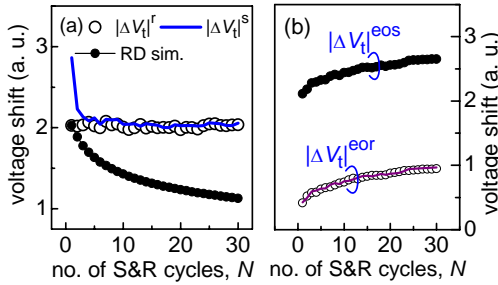


Fig. 2. Amount of change in  $|\Delta V_t|$  during stress and recovery,  $|\Delta V_t|^s$  and  $|\Delta V_t|^f$ , respectively (cf. Fig. 1), as a function of the number of stress and recovery (S&R) cycles.

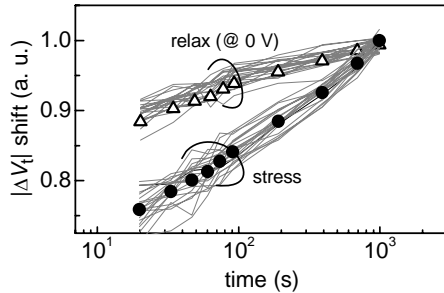


Fig. 3. Evolution of  $|\Delta V_t|$  shift during stress and recovery cycles (from 10<sup>th</sup> to 30<sup>th</sup> cycles; cf. Figs. 1 and 2) showing highly repeatable characteristics over many cycles. Symbols denote averaged curves.

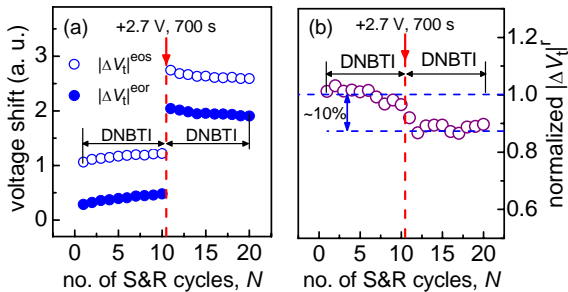


Fig. 4. Inserting a +2.7 V stress for 700 s in-between two dynamic NBTI sequences causes P to increase but R to decrease.

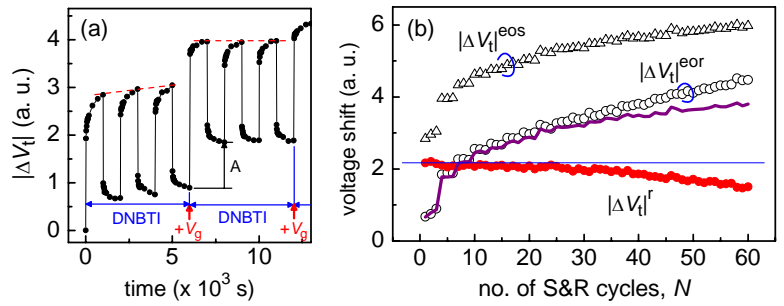


Fig. 5. (a) In this experiment, alternate dynamic NBTI (DNBTI) and positive  $V_g$  stress (+2.9 V; 5 s) were applied to the device under test. Dynamic NBTI always consisted of three stress and recovery (S&R) cycles (-1.8 V stress; 0 V recovery; stress and recovery intervals were 1000 s each) and was applied first. This was followed by the positive  $V_g$  stress and then dynamic NBTI and so on. (b)  $|\Delta V_t|$  at the end of each NBTI stress and recovery cycle,  $|\Delta V_t|^{\text{eos}}$  and  $|\Delta V_t|^{\text{eor}}$  respectively, and the amount of  $|\Delta V_t|$  recovery per cycle,  $|\Delta V_t|^f$  (cf. Fig. 1) are shown as a function of the number of S&R cycles. The thick solid line is obtained by subtracting the constant  $|\Delta V_t|^f$  of the first three recovery cycles from  $|\Delta V_t|^{\text{eos}}$ .

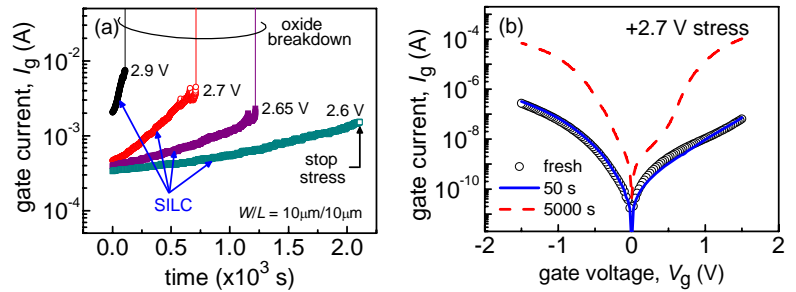


Fig. 6. (a) Evolution of gate current  $I_g$  under positive  $V_g$  stress. Significant increase in stress induced leakage current (SILC) is apparent in the later stage, which signifies substantial oxide trap generation. (b) Substantial increase in SILC is also apparent at low voltage measurement.

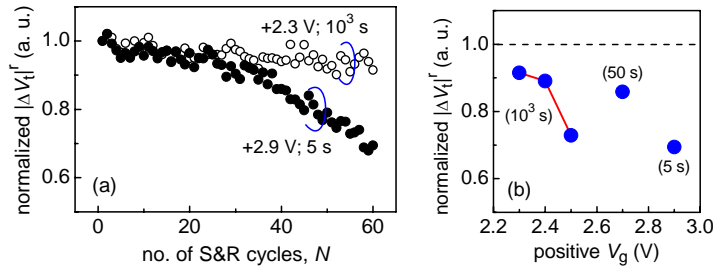


Fig. 7. (a) The reduction of  $|\Delta V_t|^f$  (normalized to that of the first recovery cycle) is shown to be sensitive to the positive  $V_g$ . (b)  $|\Delta V_t|^f$  decreases as + $V_g$  is increased; solid line is an eye guide only. For  $V_g = 2.3$  to 2.5 V, the stress interval is 1000 s. This is decreased to 50 s and 5 s, respectively, for  $V_g = 2.7$  V and 2.9 V (to avoid gate oxide breakdown). Data are extracted at the 60<sup>th</sup> S&R cycle (or after application of 20 positive  $V_g$  stress cycles).

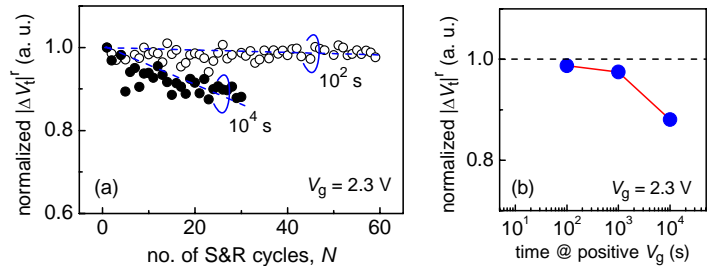


Fig. 8. For a given positive  $V_g$  stress, the reduction of  $|\Delta V_t|^f$  is shown to be sensitive to the stress time. (b)  $|\Delta V_t|^f$  decreases more significantly for longer positive  $V_g$  stress time. Data are extracted at the 30<sup>th</sup> S&R cycle (or after application of 10 positive  $V_g$  stress intervals).